Desalination and Water Treatment
www.deswater.com

doi: 10.5004/dwt.2023.30240

316 (2023) 616–626
December

Integrated membrane techniques nanofiltration/pervaporation for desalination of textile wastewater

Joanna Marszałek[a,*], Natalia Misztela[a], Renata Żyłła[b]

[a]*Faculty of Processes and Environmental Engineering, Lodz University of Technology, 223 Wólczańska str., 93-005 Łódź, Poland, Tel.: +48 42 6313700; email: joanna.marszalek@p.lodz.pl (J. Marszałek)*
[b]*Łukasiewicz Research Network, Lodz Institute of Technology, 19/57 Marii Skłodowskiej-Curie str., 90-570 Łódź, Poland, Tel.: +48 42 3070901; email: renata.zylla@lit.lukasiewicz.gov.pl (R. Żyłła)*

Received 2 October 2023; Accepted 22 December 2023

ABSTRACT

The textile industry is a sector that causes significant environmental pollution through the production of polluted wastewater. In this work, desalination tests of wastewater were carried out using a hybrid nanofiltration/pervaporation (NF/PV) system. A model textile wastewater after the dyeing process was prepared and tested at four different NaCl water solution concentrations. The properties of the obtained filtrates and concentrates (pH, conductivity, color and chemical oxygen demand (COD)) for both membrane processes were analyzed. The possibility of textile wastewater treatment using nanofiltration and pervaporation integrated processes using commercial polymer membranes was validated. For comparison, experiments with commercial ultrafiltration membrane in the pretreatment stage were performed. The performance (permeate flux and resistance) and conductivity reduction were calculated. The hydrophilicity of the membrane surfaces was measured using a method based on contact angle measurements. In the integrated NF/PV processes, each of them was considered separately. The higher the initial salt concentration in the wastewater after NF process, the lower the permeate flux passing through the membrane (62.98 to 300.8 kg/(m^2·h)), degree of conductivity reduction (16% to 48%), color (34% to 99%), and COD (81% to 97%). Fouling and concentration polarization phenomena were observed. The purified NF filtrate was then fed to the PV process for desalting. In PV, the initial various salt concentration in the wastewater did not significantly affect the permeate flux (1.18 to 1.46 kg/(m^2·h)) or the conductivity reduction, which was almost 100% in all cases. The results indicate the potential of integrated NF/PV techniques for desalination of textile wastewater from the dyeing process.

Keywords: Textile wastewater; Desalination; Membrane; Nanofiltration; Pervaporation

1. Introduction

In the era of a developing global economy, the textile industry is a sector that causes significant environmental pollution. It is estimated that by 2050, the total supply of clothing will be three times higher than it is currently, reaching approximately 160 million tons/y. High water consumption in this industry, the increasing global population, and its needs contribute to the growing demand for water. It is important to reduce its consumption, purify it, and reuse it in a closed-loop system. Chemical oxidation, ion exchange, adsorption, and membrane techniques such as ultrafiltration (UF) and nanofiltration are used to treat wastewater from the textile industry [1–17].

One of the challenges in the process of treating textile wastewater is the significant diversity of wastewater. The finishing processes of textile products involve a series of unit operations that utilize a substantial quantity of various

* Corresponding author.

Presented at the XIV Scientific Conference Membranes and Membrane Processes in Environmental Protection – MEMPEP 2023, 21–24 June 2018, Zakopane, Poland

inorganic compounds, alkalis, acids, as well as a range of organic compounds, including dyes. Depending on the type of fiber being used, different chemicals, dyes, and process conditions are employed. Each individual process aimed at dyeing, bleaching, finishing, or enhancing the functionality of textiles consequently involves the use of chemical compounds that ultimately end up in wastewater to a greater or lesser extent. As a result, textile wastewater contains both organic compounds and salts, including monovalent ions. This significantly complicates the water recovery process using membrane techniques [18–21].

To reduce fouling effects during the membrane filtration process, pretreatment methods such as coagulation or a cascading system of membrane filtration from microfiltration to reverse osmosis are used, isolating progressively smaller particles along with monovalent ions [2,21–23]. The nanofiltration process allows the removal of dye particles from fiber dyeing processes [19,20]. In some cases, an additional purification step may be necessary to achieve the required filtrate quality before it enters the next stage of membrane filtration [24,25].

Currently, reverse osmosis (RO) is widely used for desalination of seawater and brackish water. RO is characterized by high efficiency and retention of the obtained filtrate [26,27]. Research is also being conducted on the application of RO in the treatment of textile wastewater [28,29]. However, the RO process efficiency decreases at higher salt concentrations. The decrease in permeate flux is compensated by increasing hydraulic pressure. The applied hydraulic pressure must overcome the natural osmotic pressure of the feed water. Industrial produced water has often very high osmotic pressures (even above 100 bar) which necessitates the use of another purification method [30]. This raises the specific energy consumption and, in turn, the operational costs of the RO process [31]. To address the challenge of treating high-concentration brine, new membrane desalination methods are constantly being sought. In the field of water desalination, there is currently growing interest in low-pressure-driven membrane techniques, including membrane distillation (MD) and pervaporation (PV). Numerous scientific studies focus on the experimental desalination of model NaCl solutions or seawater [32,33]. To emphasize the significance of this topic, it is worth mentioning that Sulzer (DeltaMem), a Swiss Company producing PV membranes, is currently working on developing a new membrane for water desalination.

Pervaporation is a membrane technique used for special applications and small-scale industrial installations. It is known for its use in dehydrating organic solvents (including alcohols), removing diluted organic compounds from water streams, and separating organic–organic mixtures [34–35]. PV cannot compete with RO in the desalination processes of water or aqueous solutions, but it can serve as an alternative in the case of high salinity of the feed solution [32]. It can also replace another membrane technique, that is, MD.

The aim of this study was to investigate the potential application of integrated nanofiltration (NF) and pervaporation (PV) techniques for desalination of textile wastewater after the dyeing process. The proposed hybrid purification system is an experimental method not yet used in industry.

2. Materials and methods

The composition of model textile wastewater (MTW) was determined based on analyses of actual textile wastewater generated after the dyeing process of textile products [36]. Two types of dyes were used to prepare MTW in the form of an aqueous solution: reactive Helactin Red DEBN (BORUTA-ZACHEM, Poland) and direct Direct Scarlet4BS (BORUTA-ZACHEM, Poland), each at a concentration of 0.05 g/dm^3, as well as a non-ionic surfactant (fatty alcohol ethoxylates) Rucogen FWK (Rudolf Chemie, Germany) at a concentration of 0.2 g/dm^3, and NaCl at concentrations (C_0) of 0, 4, 8 and 12 g/dm^3. The chemical structures of the tested dyes were presented in a previous paper [37]. The color values (measured as absorbance at λ_{max} = 510 nm), chemical oxygen demand (COD), pH and conductivity of the feed solution (model textile wastewater) are presented in Table 1.

Flat commercial membranes were used for the NF (or ultrafiltration for comparison) and PV processes (Table 2). In the nanofiltration process, composite polyethersulfone membranes coated with a loose polyamide layer based on

Table 2
Membranes used in the study

Membrane	Membrane process	Manufacturer
NF90	NF	Dow FilmTec (USA)
HL	NF	GE Osmonics (USA)
ST	UF	Synder™ (USA)
PERVAP 2201	PV – for volatile organics and reaction mixture	Sulzer Chemtech (Switzerland)
PERVAP 2202	PV – for volatile organics and their mixture	Sulzer Chemtech (Switzerland)

Table 1
Parameters of feed solution

C_0	Conductivity	Color (λ_{max} = 510 nm)	Chemical oxygen demand	pH
(g·Na/dm^3)	(mS)	(–)	(mg·O_2/dm^3)	(–)
0	0.119	2.476	353	6.74
4	7.08	2.379	357	6.9
8	13.97	2.348	355	6.7
12	20.9	2.318	401	6.63

piperazine HL and NF90 [38] were used. For comparison, a series of experiments were performed using the ST ultrafiltration membrane (Synder™), due to the economic optimization of the filtration process. Ultrafiltration processes require lower energy inputs than nanofiltration processes, although their separation efficiency is limited. The ST membrane was made of polyethersulfone (PES) with a molar weight cut-off (MWCO) of 10,000 Da. Sulzer PERVAP 2201 and PERVAP 2202 flat, hydrophilic membranes with an active polyvinyl alcohol (PVA) layer were employed for pervaporation. Both PV membranes, in accordance with the manufacturer's specifications, were used for dehydration and separation of volatile organic substances and reaction mixtures. The manufacturer recommended their use in the PV process at a pH of feed from 5 to 8 up to a maximum temperature of 107°C. The measurement of membrane wetting angle used distilled water, 99% diiodomethane (CH_2I_2) from Alfa Aesar (USA), and formamide (CH_3NO) from Chempur (Poland).

In this study, integrated membrane techniques were applied in a sequential system, as shown in Fig. 1. Nanofiltration was used for the pretreatment of textile wastewater. In the next stage of the research, the filtrates obtained from NF were subjected to the pervaporation process to desalinate the wastewater. An exception was made for the filtrate from the ST membrane, which required additional treatment by coagulation. During the NF process, samples of filtrate solutions and their corresponding concentrates were collected at concentration ratios ranging from 0% to 50%. The calculation of the concentration ratio is given in Eq. (1).

$$\text{Concentration ratio} = \frac{\text{permeate mass}}{\text{initial mass of feed solution}} \times 100\% \quad (1)$$

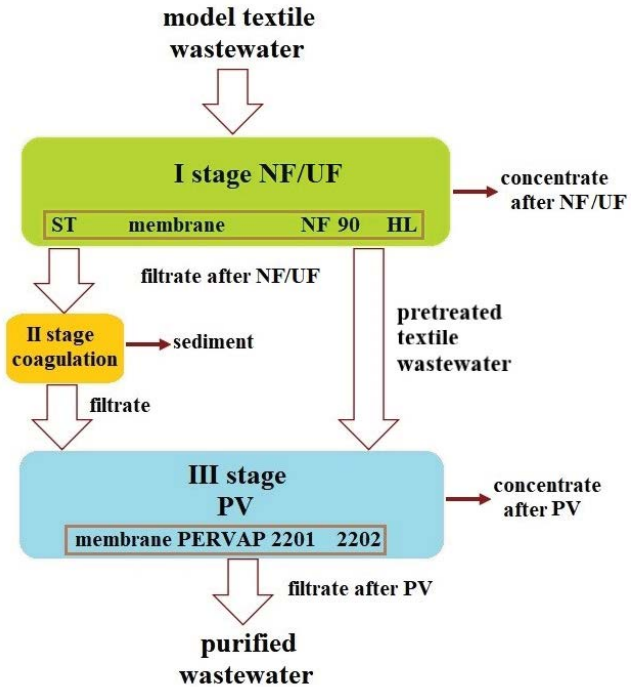

Fig. 1. Process flowchart for textile wastewater purification discussed in the work.

During the experiments, analytical tests were conducted on samples collected during NF, including measurements of mass, pH and conductivity (CPC-505 or CPC-11 Elmetron (Poland)), color (Spectrofotometer UV-VIS V-60 Jasco (Japan)) and COD (HACH Lange LT 200 (USA)). For the filtrate obtained after PV, mass and conductivity were determined. The efficiency and selectivity of the NF and PV membrane processes were calculated by determining the permeate flux (J) and retention factor of the selected parameter. The filtrate/permeate flux was calculated using Eq. (2):

$$J = \frac{mA}{t}\left[\text{kg}/\left(\text{m}^2\text{h}\right)\right] \quad (2)$$

where m – mass of the filtrate, kg; A – surface area of the membrane, m², A_{NF} = 0.008 m² for NF, A_{PV} = 0.005 m² for PV; t – time, h.

In this study, the total resistance of the liquid flow through the membrane (R_{TOT}) during the NF process was also determined according to Eq. (3). On the other hand, the total resistance is the sum of the resistance of the clean membrane (R_p) and the resistance of the fouling layer formed on the membrane during the process (R_F). Based on the total membrane resistance [Eq. (3)] obtained during the actual wastewater NF process (at a temperature of 40°C and a pressure of 0.7 MPa for ST and 1.5 MPa for NF90 and HL membranes) and the averaged resistance of pure water flow for NF under the same conditions, the fouling resistance formed on the membrane during the process was calculated. Similar considerations were made in a previous study [37].

$$R_{TOT} = \frac{\Delta P}{(J\eta)}\left[\text{m}^2/\text{kg}\right] \quad (3)$$

where ΔP is the transmembrane pressure in NF in Pa, and η is the viscosity of permeate solution, at 40°C, in Ps·s.

2.1. Nanofiltration

The nanofiltration process was conducted using a cross-flow method at 40°C, with a constant flow rate of up to 2 dm³/min and a constant pressure of 0.7 or 1.5 MPa. The setup for NF is illustrated in Fig. 2. A model feed solution with a volume of 5 dm³ was supplied to the membrane module (4) using a pump (2). The permeate (filtrate) was collected in a separate container (7), which resulted in a gradual concentration of the circulated stream, that is, the concentrate. The filtration process was carried out until the final concentration ratio reached 50%, as determined by Eq. (1).

2.2. Coagulation

The filtrate obtained in the NF process using the ST membrane required additional treatment due to insufficient removal of color from the filtered wastewater. For this purpose, a coagulant was used, which consisted of a 1% chitosan acetate solution along with NaOH solution added during mixing. The coagulation process was conducted in Imhoff funnels using a mechanical stirrer. Subsequently, the

solution was allowed to settle for 24 h to generate a flocculent sediment at the bottom of the funnels. The sediment was then decanted, resulting in a solution of decolorized wastewater, which was then directed to the next purification stage. Conductivity and spectrophotometric analyses were carried out on the filtrates after the coagulation process.

2.3. Pervaporation

The final stage of treating textile wastewater was carried out using pervaporation (PV). The PV experiments aimed at complete desalination of wastewater were conducted in a cross-flow system on a modified laboratory-scale PV unit purchased from Sulzer Chemtech.

The setup is shown schematically in Fig. 3. The feed solution was introduced into the feed tank (1) and heated to the desired temperature using a thermostat (2). It was then delivered to the membrane module (5) using a dosing pump (3). The concentrate (retentate) was returned to the tank (1), and the vaporized filtrate (permeate) was condensed in a receiver (6) immersed in liquid nitrogen (7). The pressure generated by the vacuum pump (9) on the low-pressure side of the membrane was maintained at 3 kPa. The PV experiments were conducted at 40°C. The flow rate of the feed solution was set at 40 dm^3/h. PV processes were carried out for 2.5 h with permeate samples taken every 0.5 h. The salt concentration in the collected samples was measured using a CPC-511 conductometer from Elmetron (Poland).

3. Results

3.1. Nanofiltration

The process was conducted in two stages. In the first stage, the model textile effluents were subjected to nanofiltration. In the second stage, the filtrates obtained from the nanofiltration process were directed to a pervaporation system for further purification and desalination. Fig. 4 shows the hydrodynamics of permeate (distilled water) flow across the NF90 membrane as a function of temperature and pressure. The filtration rate depends on both temperature and pressure. Many factors influence the efficiency of the filtration process. Pressure and temperature are some of the dominant factors influencing process efficiency. Water temperature has a significant effect on water density and viscosity, which affect the filtrate flux. As the viscosity and density of the filtered medium increases, the transmembrane pressure

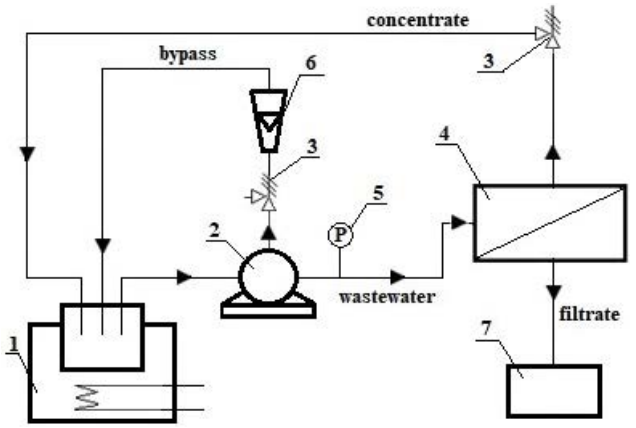

Fig. 2. Schematic diagram of the nanofiltration system: 1 – thermostat, 2 – pump, 3 – control valves, 4 – pressure chamber with the membrane, 5 – manometer, 6 – rotameter, 7 – measuring cylinder.

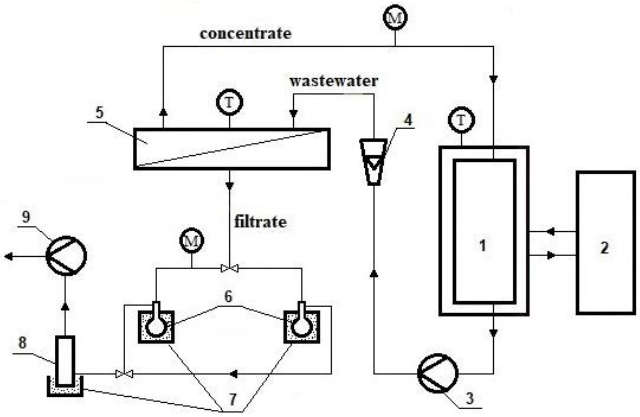

Fig. 3. Schematic diagram of the pervaporation system: 1 – feed tank, 2 – thermostat; 3 – circulation pump; 4 – flow meter, 5 – membrane module, 6 – permeate collector, 7 – liquid nitrogen cooling, 8 – drop catcher, 9 – vacuum pump.

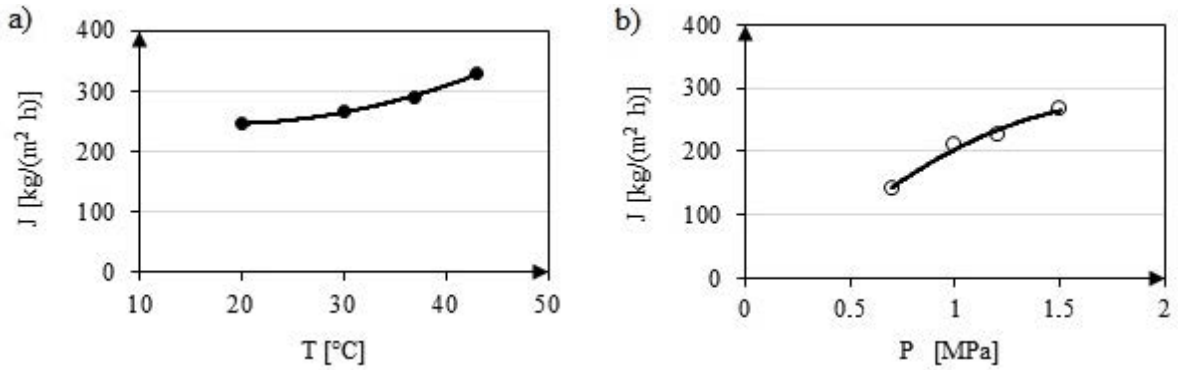

Fig. 4. Dependence of the mass flow rate of permeate for the nanofiltration process of distilled water on NF90 membrane (a) on temperature (at P = 1.5 MPa) and (b) pressure (at T = 30°C).

(TMP), which is required to force water through the membrane, also increases, resulting in a decrease in membrane permeability [39]. Transport through the membrane is driven by a pressure difference. With pressure growth the process efficiency increases. The effect also depends on several other factors, for example, the spatial structure of the membrane pores. The effect of temperature on the thermal expansion of pore sizes of commercial polymer membranes is a well-documented phenomenon [40–42]. For example, it was shown that pores of a PVDF membrane (Jiangsu Dafu Membrane Technology Co., China) with a size of 0.1 μm after increasing the water temperature from 20°C to 40°C had an average diameter increased from 0.78 to 0.88 nm [42]. Tikka et al. [41] showed that membrane pore sizes changed from 0.48 and 0.46 nm to 0.56 and 0.51 nm, respectively, by switching the feed water temperature from 5°C to 25°C. However, each type of pore may respond differently to temperature increase. Analysis of the effect of pore size is quite difficult because some membranes have a bimodal pore diameter distribution (HL), while others do not (NF90) [43–45]. Our previous studies of the NF process show that the HL membrane has the most pores with a diameter of 0.71 to 1.03 nm and relatively fewer large pores with a size of 1.3 to 2.0 nm [38]. The NF90 membrane in most publications is characterized by a dense membrane made of fully aromatic polyamide, with relatively low filtration flux and a high retention factor [46–49].

3.1.1. Contact angle

The presence of detergent in the wastewater significantly increased the hydrophilicity of NF membranes (NF90 and HL) and UF membranes (ST) (Table 3). Due to the fact that surfactants belong to amphiphilic compounds that consist of a hydrophilic head group to which a hydrocarbon chain is connected, they can affect the hydrophilicity of the membrane [50]. A characteristic property of amphiphilic substances is the formation of large aggregates (millicells) after reaching critical micellar concentration (CMC). In these micelles, the hydrophilic heads are directed towards the aqueous solution, while the hydrophobic tails are rotated in the center. Micelles can adsorb on the membrane surface, especially when nonionic surfactants are used. This may cause an increase in the hydrophilicity of the membrane in the filtration process of textile wastewater containing surfactants [51].

It was observed that the presence of NaCl in the wastewater increased the hydrophilicity of the membranes. Literature data report that in the case of ionic surfactants, after adding an electrolyte, adsorption of the surfactants increases or decreases depending on the charge of the membrane surface and the surfactant [50]. This can be explained by the weaker repulsive forces between the surfactant heads, which enables better packing of the surfactants on the membrane and thus results in a more hydrophilic surface [50].

Table 3
Averaged contact angle measurement results for membranes in the nanofiltration process

Feed/membrane	$C_{0\,NaCl}$ (g·NaCl/dm^3)	Contact angle (°)		
		NF90	HL	ST
Distilled water	–	34.0	59.0	67.69
Textile wastewater	0	30.4	47.2	50.1
	4	35.2	41.3	41.6
	8	30.3	41.8	42.6
	12	24.2	40.0	36.6

3.1.2. Nanofiltration efficiency

The curves in Fig. 5 show the dependence of the filtrate flow rate on the filtration time for various NaCl concentrations in wastewater matrices for selected membranes: nanofiltration NF90 and HL and ultrafiltration ST. Flux values are different for different membranes. For all membranes, a significant decrease in the filtrate flow rate was observed with an increase in salt concentration. This is due to concentration polarization, which involves the formation of a boundary layer of solution with a concentration exceeding the average concentration of the filtered solution, directly adjacent to the membrane. This leads to an unfavorable reduction in the process rate and a change in the separation properties of the membrane [52,53]. The most significant differences can be observed for UF membrane ST made of polyethersulfone (PES), where the flux decreased from 300 to approximately 50 kg/(m^2·h). Experiments for the ST ultrafiltration membrane were performed for comparative purposes. The retention efficiency of the surfactants as aggregates or monomers during membrane processes can vary significantly [50]. Surfactants at concentrations exceeding the critical micelle concentration (CMC) may occur in the aqueous phase in three forms: as monomers, as aggregates or adsorbed at the air/water interface [54]. The literature has documented a positive effect of surfactants on the separation of certain substances, for example, heavy metals. This may be due to the fact that detergents, after forming micelles, can form a layer on the membrane surface that interacts with some pollutants [50,51]. Cornelis et al. [51] showed that the adsorption of nonionic surfactants on the membrane surface and in the pores is the main mechanism of membrane fouling. The formation of micelles may improve the separation of compounds whose molar mass is lower than MWCO [55].

The pH values of the model wastewater subjected to nanofiltration ranged from 6.5 to 7.0. Polyamide membranes have their isoelectric point at a pH of approximately 3–4 [38]. Above this value, polyamide membranes become negatively charged, which significantly affects the membrane's ability to repel electrostatically negatively charged particles.

Fig. 6 shows the flow resistance values for NF90, HL and ST membranes. The flow resistance values are in the order of 10^{13} m^2/kg. Filtrate collection led to an increase in the concentration of substances in the influent wastewater stream, which resulted in an increase in resistance and a decrease in the process rate. With the increase in salt concentration in the model wastewater subjected to filtration, the total membrane resistance also increased. Among membranes used in the study, the HL membrane characterized by the densest structure had the highest flow resistance [38]. The values

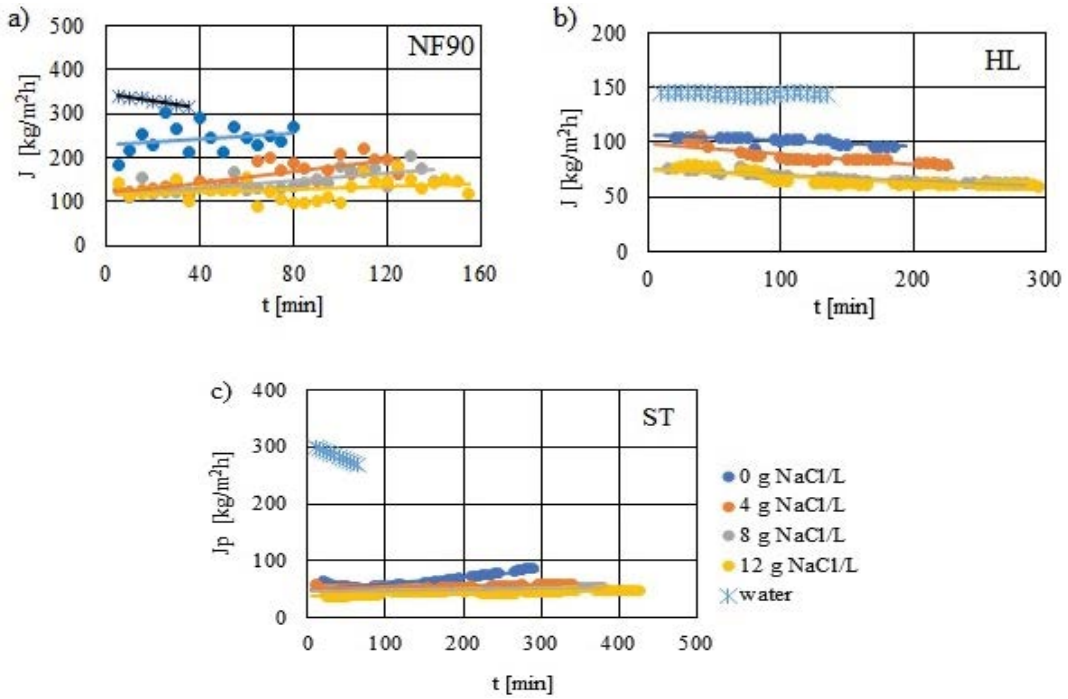

Fig. 5. Dependence of permeate mass flow rate on time for nanofiltration or ultrafiltration processes of textile wastewater with varying initial NaCl concentrations at 40°C and 1.5 MPa pressure for (a) NF90, (b) HL and (c) ST (ultrafiltration) (P = 0.7 MPa) membranes.

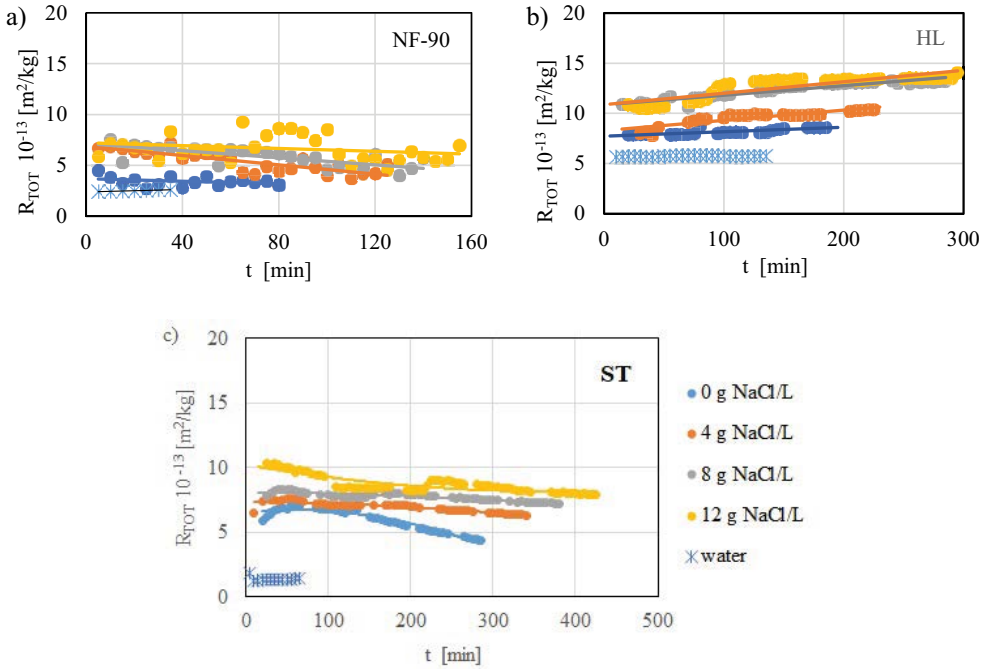

Fig. 6. Dependence of the total resistance on time for the nanofiltration or ultrafiltration processes of textile wastewater with varying initial NaCl concentrations at 40°C and 1.5 MPa pressure for (a) NF90, (b) HL and (c) ST (ultrafiltration) (P = 0.7 MPa) membranes. For distilled water ($2.5 \cdot 10^{13}$ m²/kg).

of resistance R_F calculated for the three membranes NF90, HL and ST (Fig. 7) were the highest for the HL membrane. It can be assumed that, in addition to concentration polarization, pore clogging occurred in the membrane, which significantly increased the resistance and efficiency of the process.

Fig. 8 presents the relationship between the degree of color reduction and the concentration ratio for various salt concentrations in the aqueous matrix. The results are shown for the NF90 membrane. Fig. 9 shows the relationship between the COD reduction and the concentration rate for various salt concentrations in the aqueous matrix. A similar reduction in COD was observed for the second nanofiltration membrane, HL. The color and COD reduction gradually decreased during concentrate thickening. It was observed that the presence of NaCl in the solution significantly reduced the efficiency of organic mass separation [56]. This phenomenon occurred for all tested membranes. However, in the case of the ultrafiltration membrane, an increase in the retention coefficient calculated for COD was observed during concentrate thickening.

Loosely packed nanofiltration and ultrafiltration membranes exhibited low salt retention coefficients as shown in Figs. 10 and 11. As salt concentration increased, retention coefficients decreased, although the absolute values of retained salt were similar. The obtained filtrates were directed to the pervaporation process.

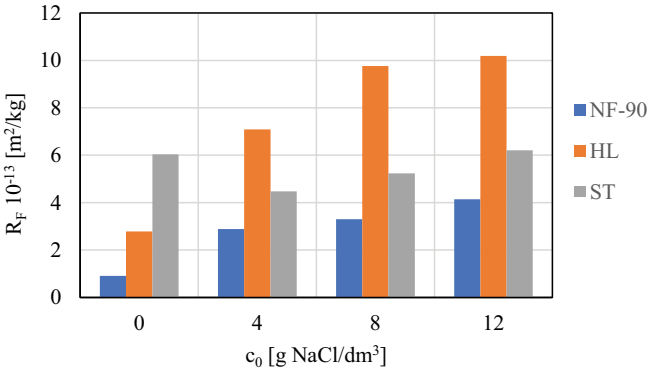

Fig. 7. Dependence of the average fouling resistance (R_F) for the nanofiltration process conducted on membranes on the initial salt content in model textile wastewater (at 40°C and under a working pressure of 1.5 MPa for NF90, HL and P = 0.7 MPa for ST (ultrafiltration) membranes.

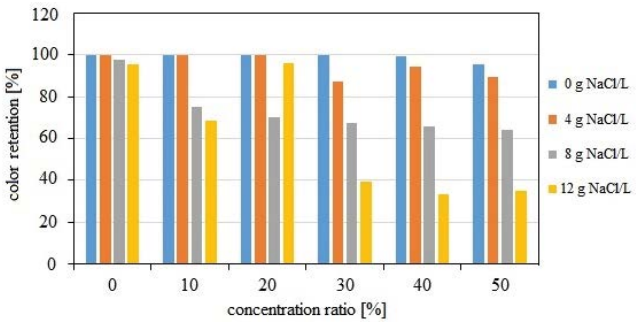

Fig. 8. Dependence of color reduction on the concentration ratio in nanofiltration processes for the NF90 membrane.

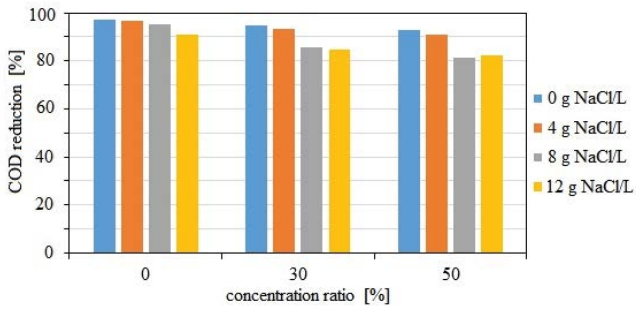

Fig. 9. Dependence of chemical oxygen demand reduction on the concentration ratio in nanofiltration processes for the NF90 membrane.

3.2. Coagulation

After the nanofiltration process on the ST membrane, a high level of filtrate coloration was obtained. Therefore,

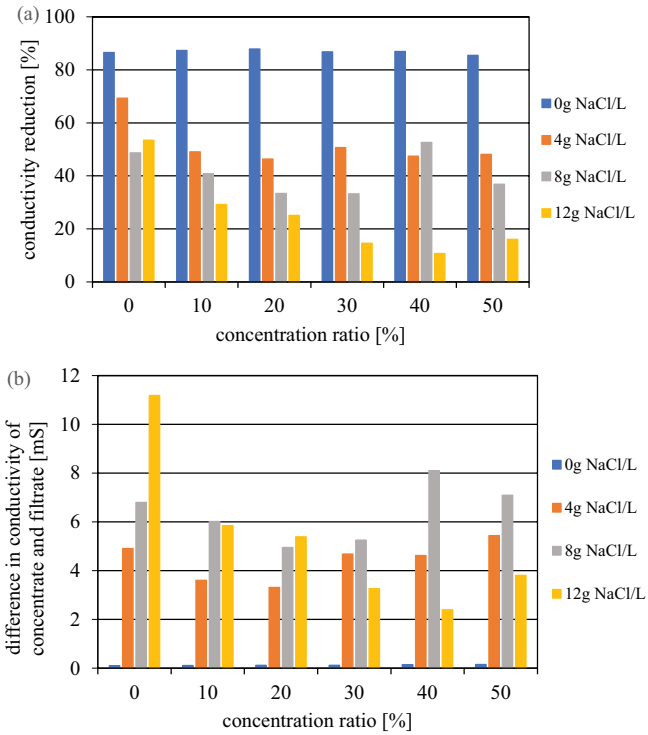

Fig. 10. Dependence of conductivity reduction on the concentration ratio in nanofiltration processes for the NF90 membrane.

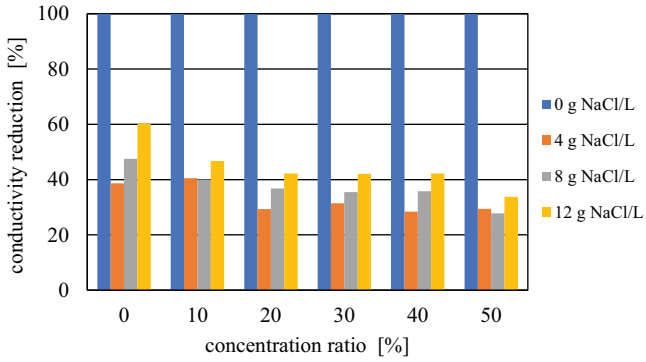

Fig. 11. Dependence of conductivity reduction on the concentration ratio in nanofiltration processes for the HL membrane.

before the pervaporation, an additional decolorization process was performed using coagulation. The results of absorbance before and after coagulation are shown in Fig. 12. Coagulation significantly reduced the color level, which could also be observed visually.

3.3. Pervaporation

In the PV process, desalination tests were performed on pretreated textile wastewater using PERVAP 2201 and PERVAP 2202 membranes. The pretreated wastewater (feed stream for PV) was produced from model textile wastewater in the NF process and coagulation as shown in the diagram presented in Fig. 1. However, the filtrate from the NF90 and HL nanofiltration membranes required desalination only in the PV stage. The NF filtrate parameters for NF90 membrane are shown in Table 4.

The research focused on determining the performance and selectivity of the pervaporation membranes used. The performance is represented by the average permeate flux (J) passing through the membrane. Selectivity is measured as the degree of conductivity reduction. The average permeate flux was calculated for a single PV process lasting 2.5 h by measuring the permeate weight every 0.5 h. The calculated intermittent fluxes stabilized with the duration of the PV process and reached an equilibrium state. The dependence of the average permeate flux (J) in the pervaporation process on the PERVAP 2201 membrane (after NF on the NF90 membrane) and the PERVAP 2202 membrane (after NF on the HL and UF on the ST membranes) on the initial NaCl concentration in textile wastewater is shown in Fig. 13. For pervaporative purification of pretreated textile wastewater at 40°C on the PERVAP 2201 membrane, after filtration in NF on the NF90 membrane, the average permeate flux (J) stabilizes with an increase in the initial NaCl content in the feed (Fig. 13).

In contrast, the permeate flux behaves differently for the pervaporation membrane PERVAP 2202. Here, one can observe a significant increase in J if the NF membrane HL was used. A slight decrease in J is, however, noticeable when the feed from the UF process on the ST membrane is introduced into the system. Such performance behavior of individual PV membranes is probably related to the degree of desalination in the NF process and thus to their selectivity. Based on the NF results, it can be seen that the HL membrane used in NF was characterized by a high, approximately 30%, conductivity reduction for all NaCl concentrations in the initial feed. Due to the hydrophilicity of the PV membranes used, mainly small solvent molecules permeated through the membrane, leaving salts on the side of the membrane at atmospheric pressure. Hence, the permeate flux decreased in the case of the feed after ultrafiltration on the ST membrane, for which the degree of color reduction and desalination was very low.

The average permeate flux (J) consistently increases with the rise in the operating temperature of the PV process, regardless of the initial feed composition, as shown in Table 5. For membranes, the flux is at a similar level and amounts to approximately 3.6 kg/(m²·h). The ratio of J at 60°C to 40°C, for the PERVAP 2202 membrane when the feed comes from NF on the HL membrane, remains close to unity as the initial salt concentration in the model wastewater increases. This indicates a minor difference between the fluxes despite the increase in PV temperature and initial salt content in the wastewater. Based on all the analyzed PV results, it can be concluded that the highest performance in the PV process was clearly achieved on the PERVAP 2202 membrane with the feed originating from the NF process on the HL membrane.

Based on the collected permeate and retentate samples, the selectivity of the pervaporation membranes used was calculated, expressed by the degree of conductivity reduction, similarly to the case of NF and UF. This parameter indicates the degree of retention of salt dissolved in the model textile wastewater. However, in the case of model textile wastewater containing substances other than salt, for example, surfactants, the conductivity cannot be directly converted to electrolyte concentration. Fig. 14 shows the degree of conductivity reduction for individual PV processes of model textile wastewater containing different initial concentrations of NaCl. The efficiency of desalination, exceeding 99%, for the PERVAP 2201 membrane is also repeated for the PERVAP 2202 membrane. This indicates almost complete desalination of pretreated textile wastewater in NF.

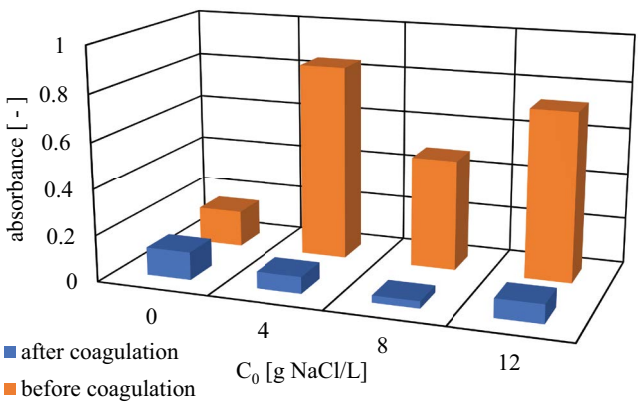

Fig. 12. Color change of nanofiltration filtrate, for ST (ultrafiltration) membrane before and after coagulation.

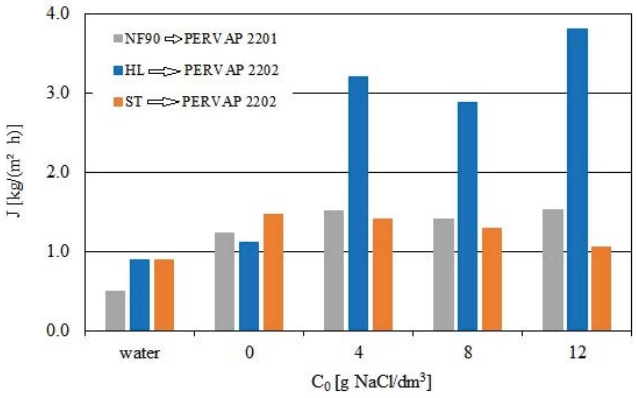

Fig. 13. Dependence of the average permeate flux (J) in the pervaporation process on PERVAP 2201 membrane (after nanofiltration on NF90 membrane) and PERVAP 2202 membrane (after nanofiltration on HL and ultrafiltration on ST membranes) on the initial NaCl concentration in textile wastewater.

Table 4
Nanofiltration filtrate parameters for NF90 membrane

C_0	Conductivity	Color (λ_{max} = 520 nm)	Chemical oxygen demand	pH
(g·NaCl/L)	(mS)	(–)	(mg·O_2/L)	(–)
0	0.027	0.002	25.7	5.77
4	5.86	0.005	30.9	5.97
8	12.16	0.017	65.4	5.96
12	19.89	0.032	111	6.61

Table 5
Comparison of permeate flux (*J*) on the PERVAP 2202 membrane at different operating temperatures of the pervaporation process for pretreated textile wastewater feed from nanofiltration on various membranes

C_0 (g·NaCl/dm^3)	Pervaporation permeate flux, *J* (kg/m^2·h)			
	After nanofiltration with HL membrane		After ultrafiltration with ST membrane and coagulation	
	40°C	60°C	40°C	60°C
0	1.12	3.53	1.46	3.74
4	3.20	3.29	1.40	3.75
8	2.88	3.69	1.29	3.67
12	3.80	4.49	1.05	3.73

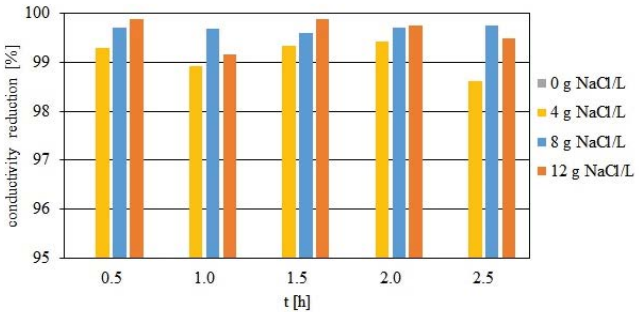

Fig. 14. Changes in the conductivity reduction during the pervaporation process at 40°C, using PERVAP 2201 membrane (feed from NF90 membrane), for various initial concentrations of textile wastewater (in g·NaCl/dm^3).

This is also evidence of the remarkable selectivity of pervaporation membranes.

4. Conclusions

In this study, desalination experiments were conducted on textile wastewater after the dyeing process using integrated NF/PV processes. The experiments were carried out with two commercial NF membranes (NF90, HL), one commercial UF membrane (ST) and two PV membranes (PERVAP 2201 and PERVAP 2202). In terms of performance and selectivity, the best NF membrane was HL Sterlitech (USA), and in the case of PV, the PERVAP 2202 membrane was the best.

Higher initial salt concentrations in the wastewater before NF resulted in lower filtrate flux through the membrane during the NF process and higher membrane resistance. This may be due to the greater resistance resulting from the concentration polarization on the membrane surface. The phenomenon of concentration polarization causes the formation of a boundary layer of a solution, in the immediate vicinity of the membrane with a concentration higher than the average concentration of the filtered solution. This causes an unfavorable reduction in the process efficiency and a change in the separation properties of the membrane.

In the case of PV, higher process temperature led to higher process efficiency. The selectivity, controlled by the degree of salt reduction, was very high (>99.9%). However, in the future, attention should be paid to the selection of an appropriate membrane that will enhance the process efficiency (flux) and achieve single-stage color reduction. The reuse of recovered water, for example, in dyeing processes, would reduce water consumption in the textile industry, which in turn would have a positive impact on the natural environment.

The experiments described in the article are aimed, among others, at minimizing the amount of hazardous membrane modules deposited in landfills or at sending them for incineration. The recovered filtrate can be reused for dyeing baths. The retentate should be sent for disposal where various chemical oxidation, coagulation or biological processes can be used. An alternative may be physicochemical processes, for example, precipitation/combustion of sediments or the Fenton process.

The results obtained in the article indicate the high potential of integrated NF/PV techniques for the desalination of textile wastewater from the dyeing process, although further research development of more efficient hydrophilic membranes may be necessary, especially for PV due to the low permeate flux.

Symbols

A	—	Membrane area, m^2
C	—	Salt concentration in the sample, g·NaCl/dm^3
J	—	Permeate flux, kg/(m^2·h)
m	—	Permeate mass, kg
P	—	Transmembrane pressure, Pa
R	—	Resistance, m^2/kg
t	—	Process time, h
T	—	Temperature, °C
η	—	Dynamic viscosity, Pa s

Indices

F	—	Fouling
p	—	Pure
TOT	—	Total
0	—	Initial

References

[1] F. Amalina, A.S.A. Razak, S. Krishnan, A.W. Zularisam, M. Nasrullah, Dyes removal from textile wastewater by agricultural waste as an absorbent – a review, Cleaner Waste Syst., 3 (2022) 100051, doi: 10.1016/j.clwas.2022.100051.

[2] T.A. Aragaw, F.M. Bogale, Role of coagulation/flocculation as a pretreatment option to reduce colloidal/bio-colloidal fouling in tertiary filtration of textile wastewater: a review and future outlooks, Front. Environ. Sci., 11 (2023) 1142227, doi: 10.3389/fenvs.2023.1142227.

[3] N. Bhargava, N. Bahadur, A. Kansal, Techno-economic assessment of integrated photochemical AOPs for sustainable treatment of textile and dyeing wastewater, J. Water Process Eng., 56 (2023) 104302, doi: 10.1016/j.jwpe.2023.104302.

[4] M. Bilińska, L. Bilińska, M. Gmurek, Homogeneous and heterogeneous catalytic ozonation of textile wastewater: application and mechanism, Catalysts, 13 (2023) 6, doi: 10.3390/catal13010006.

[5] L.A. Castillo-Suárez, A.G. Sierra-Sánchez, I. Linares-Hernández, V. Martínez-Miranda, E.A. Teutli-Sequeira, A critical review of textile industry wastewater: green technologies for the removal of indigo dyes, Int. J. Environ. Sci. Technol., 20 (2023) 10553–10590.

[6] E.B. Ingrassia, E.S. Lemos, L.B. Escudero, Treatment of textile wastewater using carbon-based nanomaterials as adsorbents: a review, Environ. Sci. Pollut. Res., 30 (2023) 91649–91675.

[7] N. Jahan, M. Tahmid, A.Z. Shoronika, A. Fariha, H. Roy, N. Pervez, Y. Cai, V. Naddeo, M.S. Islam, A comprehensive review on the sustainable treatment of textile wastewater: zero liquid discharge and resource recovery perspectives, Sustainability (Switzerland), 14 (2022) 15398, doi: 10.3390/su142215398.

[8] P. Jin, J. Zheng, Q. Gao, A.K. An, J. Zhu, B. Van der Bruggen, Loose nanofiltration membranes for the treatment of textile wastewater: a review, J. Membr. Sci. Res., 8 (2022) 538529, doi: 10.22079/JMSR.2022.538529.1492.

[9] C.G. Malar, K. Sathya, S. Rajalakshmi, P.R. Lakshmi, A critical analysis of the nanotechnology-based approach in textile wastewater treatment, Nanotechnol. Environ. Eng., 8 (2023) 535–548.

[10] G. Nair, B. Soni, M. Shah, A comprehensive review on electro-oxidation and its types for wastewater treatment, Groundwater Sustainable Dev., 23 (2023) 100980, doi: 10.1016/j.gsd.2023.100980.

[11] S. Najari, M. Delnavaz, D. Bahrami, Application of electrocoagulation process for the treatment of reactive blue 19 synthetic wastewater: evaluation of different operation conditions and financial analysis, Chem. Phys. Lett., 832 (2023) 140897, doi: 10.1016/j.cplett.2023.140897.

[12] P.V. Nidheesh, G. Divyapriya, F. Ezzahra Titchou, M. Hamdani, Treatment of textile wastewater by sulfate radical based advanced oxidation processes, Sep. Purif. Technol., 293 (2022) 121115, doi: 10.1016/j.seppur.2022.121115.

[13] A.S. Reddy, S. Kalla, Z.V.P. Murthy, Textile wastewater treatment via membrane distillation, Environ. Eng. Res., 27 (2022) 210228, doi: 10.4491/eer.2021.228.

[14] L. Rendón-Castrillón, M. Ramírez-Carmona, C. Ocampo-López, F. González-López, B. Cuartas-Uribe, J.A. Mendoza-Roca, Treatment of water from the textile industry contaminated with indigo dye: a hybrid approach combining bioremediation and nanofiltration for sustainable reuse, Case Stud. Chem. Environ. Eng., 8 (2023) 100498, doi: 10.1016/j.cscee.2023.100498.

[15] H. Tiwari, R.K. Sonwani, R.S. Singh, Bioremediation of dyes: a brief review of bioreactor performance, Environ. Technol. Rev., 12 (2023) 83–128.

[16] V. Vaiano, I. De Marco, Removal of azo dyes from wastewater through heterogeneous photocatalysis and supercritical water oxidation, Separations, 10 (2023) 230, doi: 10.3390/separations10040230.

[17] M. Yaqub, M.D. Celebi, M. Dilaver, S.K. Bhagat, M. Kobya, W. Lee, Treating textile wastewater to achieve zero liquid discharge: a comprehensive techno-economic analysis, Water Air Soil Pollut., 234 (2023) 651, doi: 10.1007/s11270-023-06646-5.

[18] L. Xu, Z. Pang, H. Yu, M. Guo, X. Yan, X. Jiang, L. Yu, Antifouling loose nanofiltration membranes prepared via the fast co-deposition of capsaicin-mimic/polydopamine for efficient dye/salt separation, Desalination, 565 (2023) 116809, doi: 10.1016/j.desal.2023.116809.

[19] L. Wang, M. Zhang, Y. Shu, Q. Han, B. Chen, B. Liu, Z. Wang., C.Y. Tang, Precisely regulated in-plane pore sizes of Co-MOF nanosheet membranes for efficient dye recovery, Desalination, 567 (2023) 116979, doi: 10.1016/j.desal.2023.116979.

[20] S. Shang, G. Xiao, C. Chen, C. Chen, R. Li, Z. Yang, M. Cao, R. Zou, Y. Tang, Constructed "sandwich" structure to obtain recyclability and high rejection rate high-flux CA@HMSN@h-BN/PDA membrane for efficient treatment of dye wastewater, Colloids Surf., A, 675 (2023) 132023, doi: 10.1016/j.colsurfa.2023.132023.

[21] A. Ahsan, F. Jamil, M.A. Rashad, M. Hussain, A. Inayat, P. Akhter, A.H. Al-Muhtaseb, K.-Y.A. Lin, Y.K. Park, Wastewater from the textile industry: review of the technologies for wastewater treatment and reuse, Korean J. Chem. Eng., 40 (2023) 2060–2081.

[22] D. Christian, A. Gaekwad, H. Dani, M.A. Shabiimam, A. Kandya, Recent techniques of textile industrial wastewater treatment: a review, Mater. Today Proc., 77 (2023) 277–285.

[23] A. Azanaw, B. Birlie, B. Teshome, M. Jemberie, Textile effluent treatment methods and eco-friendly resolution of textile wastewater, Case Stud. Chem. Environ. Eng., 6 (2022) 100230, doi: 10.1016/j.cscee.2022.100230.

[24] I. Ćurić, D. Dolar, Investigation of pretreatment of textile wastewater for membrane processes and reuse for washing dyeing machines, Membranes, 12 (2022) 449, doi: 10.3390/membranes12050449.

[25] M.D. Çelebi, M. Dilaver, M. Kobya, A study of inline chemical coagulation/precipitation-ceramic microfiltration and nanofiltration for reverse osmosis concentrate minimization and reuse in the textile industry, Water Sci. Technol., 84 (2021) 2457–2471.

[26] Y. Okamoto, J.H. Lienharda, How RO membrane permeability and other performance factors affect process cost and energy use: a review, Desalination, 470 (2019) 114064, doi: 10.1016/j.desal.2019.07.004

[27] D. Zarzo, D. Prats, Desalination and energy consumption. What can we expect in the near future?, Desalination, 427 (2018), doi: 10.1016/j.desal.2017.10.046.

[28] R. Partal, I. Basturk, S.M. Hocaoglu, A. Baban, E. Ecem Yilmaz, Recovery of water and reusable salt solution from reverse osmosis brine in textile industry: a case study, Water Resour. Ind., 27 (2022) 100174, doi: 10.1016/j.wri.2022.100174.

[29] N.B. Amar, N. Kechaou, J. Palmeri, A. Deratani, A. Sghaier, Comparison of tertiary treatment by nanofiltration and

reverse osmosis for water reuse in denim textile industry, J. Hazard. Mater., 170 (2009) 111–117.
[30] D.M. Davenport, A. Deshmukh, J.R. Werber, M. Elimelech, High-pressure reverse osmosis for energy-efficient hypersaline brine desalination: current status, design considerations, and research needs. Environ. Sci. Technol. Lett., 5 (2018) 467–475.
[31] A.J. Karabelas, C.P. Koutsou, M. Kostoglou, D.C. Sioutopoulos, Analysis of specific energy consumption in reverse osmosis desalination processes, Desalination, 431 (2018) 15–21.
[32] Y. Li, E.R. Thomas, M. Hernandez Molina, S. Mann, W.S. Walker, M.L. Lind, F. Perreault, Desalination by membrane pervaporation: a review, Desalination, 547 (2023) 116223, doi: 10.1016/j.desal.2022.116223.
[33] W. Kaminski, J. Marszałek, E. Tomczak, Water desalination by pervaporation – comparison of energy consumption, Desalination, 433 (2018) 89–93.
[34] A. Basile, A. Figoli, M. Khayet, Pervaporation, Vapour Permeation and Membrane Distillation, Woodhead Publishing Series in Energy, 2015.
[35] T. Zhu, Q. Xia, J. Zuo, S. Liu, X. Yu, Y. Wang, Recent advances of thin film composite membranes for pervaporation applications: a comprehensive review, Adv. Membranes, 1 (2021) 100008, doi: 10.1016/j.advmem.2021.100008.
[36] R. Żyłła, J. Sójka-Ledakowicz, K. Michalska, L. Kos, S. Ledakowicz, Effect of UV/H_2O_2 oxidation on fouling in textile wastewater nanofiltration, Fibres Text. East. Eur., 20 (2012) 99–104.
[37] J. Marszałek, R. Żyłła, Recovery of water from textile dyeing using membrane filtration processes, Processes, 9 (2021) 1833, doi: 10.3390/pr9101833.
[38] R. Żyłła, M. Foszpańczyk, I. Kamińska, M. Kudzin, J. Balcerzak, S. Ledakowicz, Impact of polymer membrane properties on the removal of pharmaceuticals, Membranes, 12, (2022) 150, doi: 10.3390/membranes12020150.
[39] L. Cui, G. Carl, G. Wa, B.W. Liao, Effect of cold water temperature on membrane structure and properties, J. Membr. Sci., 540 (2017) 19–26.
[40] R.R. Sharma, R. Agrawal, S. Chellam, Temperature effects on sieving characteristics of thin-film composite nanofiltration membranes: pore size distributions and transport parameters, J. Membr. Sci., 223 (2003) 69–87.
[41] A. Tikka, W. Gao, B. Liao, Reversibility of membrane performance and structure changes caused by extreme cold water temperature and elevated conditioning water temperature, Water Res., 151 (2019) 260–270.
[42] B. Xu, W. Gao, B. Liao, W. Turek, The influence of temperature on dynamic membrane structure, J. Membr. Sci., 688 (2023) 122121, doi: 10.1016/j.memsci.2023.122121.
[43] K. Kosutic, D. Dolar, D. Asperger, B. Kunst, Removal of antibiotics from a model wastewater by RO/NF membranes, Sep. Purif. Technol., 53 (2007) 244–249.
[44] D. Dolar, K. Kosutic, B. Vučić, RO/NF treatment of wastewater from fertilizer factory - removal of fluoride and phosphate, Desalination, 265 (2011) 237–241.
[45] D. Dolar, S. Pelko, K. Košutić, A.J. Horvat, Removal of anthelmintic drugs and their photodegradation products from water with RO/NF membranes, Process Saf. Environ. Prot., 90 (2012) 147–152.
[46] J.V. Nicolini, C.P. Borges, H.C. Ferraz, Selective rejection of ions and correlation with surface properties of nanofiltration membranes, Sep. Purif. Technol., 171 (2016) 238–247.
[47] E.I. Mouhoumed, A. Szymczyk, A. Schäfer, L. Paugam, Y.H. La, Physico-chemical characterization of polyamide NF/RO membranes: insight from streaming current measurements, J. Membr. Sci., 461 (2014) 130–138.
[48] N. Hilal, H. Al-Zoubi, N. Darwish, A.W. Mohammad, Characterisation of nanofiltration membranes using atomic force microscopy, Desalination, 177 (2005) 187–199.
[49] J.M. Gozálvez-Zafrilla, D. Sanz-Escribano, J.C. García, Nanofiltration of secondary effluent for wastewater reuse in the textile industry, Desalination, 222 (2008) 272–279.
[50] K. Boussu, A. Belpaire, A. Volodin, C. Van Haesendonck, P. Van der Meeren, C. Vandecasteele, B. Van der Bruggen, Influence of membrane and colloid characteristics on fouling of nanofiltration membranes, J. Membr. Sci., 289 (2007) 220–230.
[51] G. Cornelis, B. Van der Bruggen, C. Vandecasteele, I. Devreese, Fouling of nanofiltration and T membranes applied for wastewater regeneration in the textile industry, Desalination, 175 (2005) 111–119.
[52] A.S. Chugunov, V.A. Vinnitskii, K.V. Stepanyuk, Effect of the sodium chloride–magnesium chloride ratio on the separation of salts using a nanofiltration membrane, Membr. Membr. Technol., 3 (2021) 192–197.
[53] M. Qadir, G. Sposito, C.J. Smith, J.D. Oster, Reassessing irrigation water quality guidelines for sodicity hazard, Agric. Water Manage., (2021) 107054, doi: 10.1016/j.agwat.2021.107054.
[54] R.F. Nunes, H. Conceição Ferraz, F. de Araujo Kronemberger, Interaction between surfactants of different classes and nanofiltration membranes, Sci. Plena, 18 (2022) 11420, doi: 10.14808/sci.plena.2022.11420.
[55] A. Yusaf, M. Usman, M. Ibrahim, A. Mansha, A. ul Haq, H.F. Rehman, M. Ali, Mixed micellar solubilization for procion blue MxR entrapment and optimization of necessary parameters for micellar enhanced ultrafiltration, Chemosphere, 313 (2023) 137320, doi: 10.1016/j.chemosphere.2022.137320.
[56] Y.-H. Tong, Y. Wu, Z. Xu, L.-H. Luo, R. Jia, R. Han, S.-J. Xu, Hydrolysis co-deposition of bio-inspired hybrid hydrophilic network antifouling loose nanofiltration membrane for effective dye/salt separation, J. Membr. Sci., (2023), doi: 10.2139/ssrn.4638997.